JOURNAL OF GEOPHYSICAL RESEARCH, VOL. 87, NO. A8, PAGES 6053–6059, AUGUST 1, 1982

Observations of Structuring in the Downstream Region of a Large Spherical Model in a Laboratory Simulated Solar Wind Plasma

D. S. INTRILIGATOR[1]

Physics Department, University of Southern California, Los Angeles, California 90007

G. R. STEELE

Carmel Research Center, Santa Monica, California 90406

Laboratory experiments have been performed that show the effects of inserting a spherical conducting model, large in comparison with the Debye length, into a free streaming high-energy (1 kV) unmagnetized hydrogen plasma. These experiments are the first laboratory measurements at energies and compositions directly relevant to solar wind and astrophysical plasma phenomena. The incident plasma parameters were held constant. Transverse profiles of the net Langmuir probe current, plotted at various locations downstream in the model wake, are divided into three regions—the 'shadow,' the 'transition,' and the 'boundary.' The following new results are obtained: (1) enhancements in the 'shadow' exist at downstream locations where the Mach ratio is less than one; (2) turbulence exists in the 'transition' region on the shadow edges and outside in the 'boundary' region. These results appear to be attributable to the use of a high-energy plasma for these studies. A small current enhancement is also present in the boundary and is attributable to the plasma/model interaction, in close agreement with low-energy plasma/model interaction experiments. We speculate that many similar features observed by in situ spacecraft downstream from planetary bodies are relatively permanent and are due to the intrinsic nature of the interaction between the solar wind plasma and the obstacle rather than to transitory effects caused by the presence of discontinuities or other transitory characteristics associated with the flow.

INTRODUCTION

There has been considerable interest in theoretical and experimental research associated with plasma flow past bodies. However, the results are fragmentary both for laboratory and for in situ space experiments. Moreover, such experiments have emphasized the low-energy plasma flow associated with the earth's ionosphere [*Hester and Sonin*, 1969; *Oran et al.*, 1974; *Fournier and Pigache*, 1975; *Stone*, 1981*a*, *b*] rather than the high-energy flow associated with astrophysical plasmas (e.g., the solar wind, stellar winds, etc.). The previous laboratory experiments employed argon or other inert gases rather than hydrogen, one of the most common constituents of astrophysical plasmas.

In the University of Southern California (USC) Astrophysical Plasma Laboratory we took a more realistic approach in simulating the effects associated with obstacles in an interplanetary/astrophysical environment. We developed a large facility to enable the use of models, large in comparison with the Debye length, in a high-energy free streaming plasma. Figure 1 is a schematic of the major components of the facility: the large vacuum chamber, the high-energy plasma source, and the detectors.

A steady state (non-pulsed) high-energy plasma source, using injected hydrogen gas for proton production and capable of producing a stable high density plasma with well controlled and repeatable parameters, was designed and developed for the facility. The transverse uniformity of the beam was optimized. At $z/a = 2.5$ (where a is the model radius, 4.1 cm) downstream from the model location the ambient plasma beam was determined to be flat, within $\pm 10\%$ of maximum current for a transverse distance greater than ± 8 cm ($\pm 2a$) from the model center line. At z/a locations further downstream the transverse distance over which the beam remains flat increases proportionally with the divergence of the beam. This uniformity was not achieved in some low-energy plasma interaction experiments [*Hester and Sonin*, 1969].

The experimental models and detectors were designed and constructed to withstand operating potentials of several kilovolts to allow for diagnostics of the high-energy plasma. Extensive measurements were then made of the source characteristics and the plasma parameters following methods similar to those described in *Hall et al.* [1965] and *Sellen et al.* [1965] and *Schott* [1968].

The source produced a well controlled and repeatable high energy, collision free hydrogen plasma with the undisturbed plasma density decreasing as $1/r^2$ (where r is the axial distance downstream from the source), an indication of the collision free status of the beam. The undisturbed plasma upstream and downstream from the planned model location was measured repeatedly to ensure reproducible plasma parameters. Then a large spherical model ($a/\lambda_d \approx 8$, where λ_d is the Debye length) was inserted into the plasma and the incident (upstream) plasma and the downstream plasma were repeatedly mapped.

In this paper we present the resulting measured net current profiles in the wake regions from z/a of 1.2 to 8.1 for a large conducting body at zero potential with reference to the plasma. We compare these results to the findings of *Hall et al.* [1964], *Henderson and Samir* [1967], *Hester and Sonin* [1969], *Fournier and Pigache* [1975], *Grabowski and Fischer* [1975], *Samir et al.* [1974], and *Stone* [1981*a*, *b*]. All of the

[1] Also affiliated with the Carmel Research Center, Santa Monica, California 90406.

Paper number 2A0624.
0148-0227/82/002A-0624$05.00

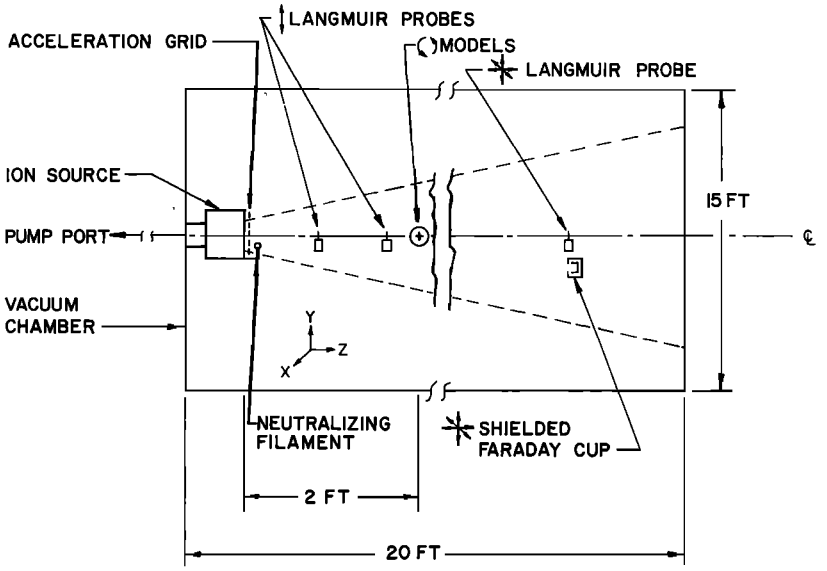

Fig. 1. A schematic of the USC Astrophysical Plasma Laboratory plasma facility, showing the locations of various detectors, the hydrogen plasma source, and the models.

data refer to the model radius $a = 4.1$ cm and were taken under the plasma conditions listed in Table 1.

Plasma Facility Description

The USC Astrophysical Plasma Laboratory contains a large plasma facility 20 feet long and 15 feet in diameter (see Figure 1). The vacuum chamber operating pressure of $<5 \times 10^{-6}$ Torr is maintained with a 36 inch diffusion pump. The 1-2 kV free streaming hydrogen plasma, formed by utilizing a modified Kaufman ion source with a finely regulated flow of hydrogen gas to control proton (H^+) production, is neutralized by using a hot filament immersed in the plasma [*Bernstein and Sellen,* 1963] at a distance of $1R_0 \approx 5$ cm (the radius of the extraction grid on the source) in front of the source.

At a position 61 cm downstream from the source the plasma is incident upon a highly polished aluminum sphere with a diameter much larger than the Debye length. The model can be moved into and out of the beam from outside the vacuum chamber by using mechanical vacuum feedthroughs. Its position is read electrically and displayed on a digital voltmeter. Thus, all the plasma parameters can be measured with and without the model in the beam. The parameters measured without the model were used as a baseline to enable accurate analysis of the model wake perturbations.

A Langmuir probe [*Langmuir and Mott-Smith,* 1924], consisting of a looped wire 1.5 cm long by 0.008 cm diameter (similar to those described in *Hall et al.* [1965] and *Sellen et al.* [1965]), floats at the plasma potential (as determined by the point where the *ln I/V* curve deviates from a straight line) and is stepped in bias voltage to obtain a *ln I/V* curve. It is mounted on a three axis translator downstream of the model, enabling us to obtain three-dimensional maps of the model wake from $z/a = 1.2$ out to $z/a = 80$ for the model. This allows us to directly compare our data with those published previously by others. The x and y locations of the probe are varied electrically and measured with integral potentiometers and displayed on a digital voltmeter with an accuracy of $\pm 0.1\%$. The z location is varied mechanically by the use of a shaft inserted through a sliding vacuum seal in the chamber wall and was measured by using a scale on the shaft. The probe current reading is the net measured current. Thus it is indicative of the ion and electron densities and fluxes.

Plasma parameters are measured for control purposes by using three separate detectors. Two of the probes are hot wire Langmuir probes mounted at $z/a = -1.3$ and $z/a = -8.4$ upstream from the model location (all probe locations are referenced to the model center line, where $z = 0$) and are mechanically moved into and out of the beam from outside the vacuum chamber. The third detector, a Faraday cup with secondary suppression capabilities and a 1 cm^2 aperture, is located on the translator directly below the Langmuir probe with the aperture in the same plane as the Langmuir probe. A gold plated tungsten grid with 80% transmission is placed across the aperture of the cup and grounded to help shield the internal fields from the surrounding plasma. This cup was calibrated by using a second larger Faraday cup (an 'absolute' cup) that was designed so that any measurements taken with it are 'absolute' in the sense described below.

The absolute cup is shielded, ~25 cm in diameter and 100 cm long, with an external aperture of 1 cm^2 and an internal

TABLE 1. Laboratory and Solar Wind Free Stream Parameters

Parameter	Solar Wind At Venus	Laboratory
Velocity (km/s), V_i	300–700	500
Density (ions/cm^3), N_i	20–40	10^7
Ion temperature (°K), T_i	$1–5 \times 10^4$	10^4
Ion composition	H^+	H^+
Electron temperature* (°K), T_e	$1–5 \times 10^5$	2×10^5
T_e/T_i	>1	>1
Debye length (cm), $\lambda_d = 6.9\,(T_e/N_e)^{1/2}$	$>10^2$	$3–6 \times 10^{-1}$
Ion acoustic Mach no., $M = V_i/(2kT_e/M_i)^{1/2}$	6	9
Debye ratio, a/λ_d	$\gg 1$	8
Model radius (cm), a	6.1×10^8	4.1
Plasma potential (V)		~0

*T_e was determined by using conventional methods associated with *I/V* curves, the straight section of our *ln I/V* plot was greater than one order of magnitude.

aperture of 1.5 cm^2. The outer shield is operated at ground potential. The size and internal structure minimize the need for secondary suppression. The cup, constructed without internal grids which would reduce the total transmission of particles entering the entrance aperture and collected by the cup, has been employed since 1967 in the laboratory calibrations of our flight plasma analyzers (e.g., the NASA Ames plasma analyzers on Pioneer 7, 8, 9, 10, 11, and the Pioneer Venus orbiter). Its characteristics have been measured many times, and we refer to its output as the 'absolute' plasma parameters. The large size of the absolute cup precludes our leaving it in the chamber during the wake studies. Initially, the output of the two cups were recorded simultaneously and used as a calibration of the smaller cup so that reliable data could be derived from it. The absolute cup was then removed from the translator and the Langmuir probes installed.

All detector outputs are monitored with sensitive laboratory electrometers to ensure that any changes in the plasma due to source or pressure fluctuations are measured. This enables us to ascertain if there is any extraneous noise in the ambient plasma. When noise is present, the plasma source is readjusted and the baseline measurements retaken. If noise occurs during a data scan, those data are disregarded and the scan is repeated.

Observations

The plasma parameters listed in Table 1 were maintained at their respective values throughout the entire data series presented in this paper. The profiles shown in Figures 2–5 are indicative of the plasma ion and electron densities and fluxes and are analogous to the current density profiles shown in *Stone* [1981*a*, *b*] but are shown as measured net currents to give the reader a better appreciation of the shadow structuring. Before and after each sequence of transverse scans, consisting of from two to four different z/a locations, the model was removed from the plasma and the ambient plasma parameters were measured to establish baseline values. The comparisons of the baseline values were made by the same detector using the same electrometer, and the maximum deviation was ±5%.

Figure 2 shows a series of transverse net current profiles taken at various locations in z, from $z/a = 1.2$ through $z/a = 8.1$ as denoted by the numbers above each profile, downstream from a model. As indicated in Figure 2, the separation in z/a between the first two profiles is only 0.1, whereas the z/a separation between the other profiles is 0.3 except between 2.8 and 3.2, 6.8 and 7.2, and 7.5 and 8.1. The vertical axis covers many orders of magnitude (from $+10^{-8}$ A to -10^{-8} A, where a net current of $\pm 1 \times 10^{-12}$ amps was chosen as the background or zero current level). The recorded currents, as read from the electrometer, changed polarity abruptly as they passed through the region of zero net probe current. When this occurred the electrometer scale polarity was changed and the zero rechecked before the data taking continued. Several transverse scans, with both the model in and out of the plasma, were taken at each z/a location to ensure repeatability and each of the contour plots is the approximate average of all the data scans for that particular location with the model in the plasma (the structures were present in all the 'model in' scans).

The horizontal axis is a dimensionless parameter x/a, with zero as its center and a range of ±3. This parameter was employed to enable us to compare our results directly with other published data [*Hester and Sonin*, 1969; *Oran et al.*, 1974; *Fournier and Pigache*, 1975; *Stone*, 1981*a*, *b*]. The x locations were recorded with the corresponding measured currents in a step and pause procedure. An electrical control system was used to move the detector along the transverse axis (x) in 0.25 cm steps. After each step the electrometer zero was checked, reset if necessary, and the output allowed to stabilize for approximately 30 s.

Figure 3 shows two current profiles taken at $z/a = 2.8$ with the same vertical and horizontal axes as those in Figure 2. Three separate regions of interest (shadow, boundary, and transition) are defined for the profile with the model in the plasma (solid line). The dashed line profile is the ambient plasma current with the model removed. It shows that for a transverse distance greater than $\pm 2a$ the plasma beam was

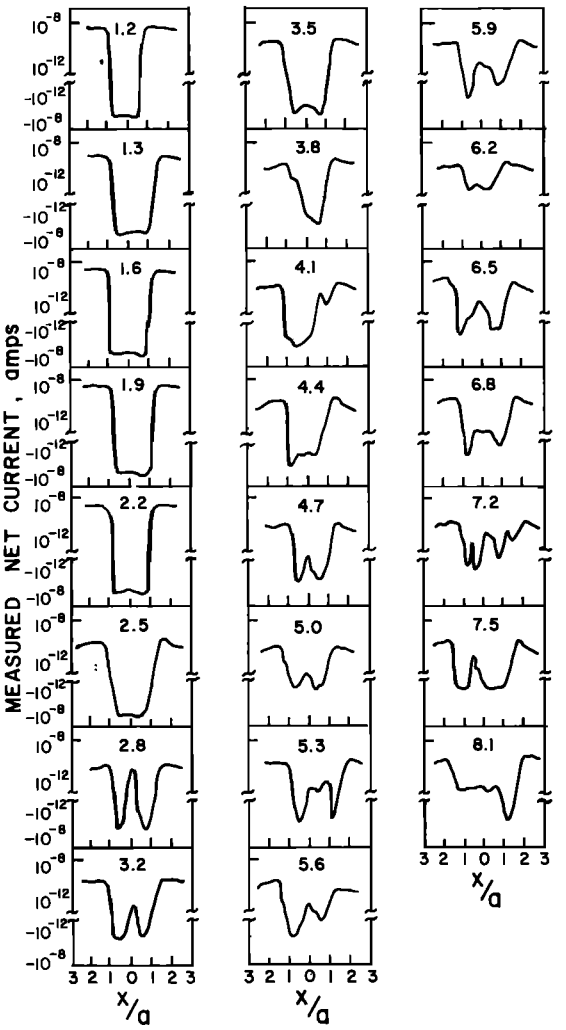

Fig. 2. A series of transverse net current profiles measured downstream of a large ($a/\lambda_d = 8$) conducting spherical model. The vertical axes are the measured net current. Each axis covers many orders of magnitude ranging from $+10^{-8}$ A to -10^{-8} A. The zero net current levels are $\pm 10^{-12}$ A and the vertical scales have been broken at these locations. The horizontal axis is the dimensionless number x/a with an amplitude of ±3, where x is the transverse location and a is the model radius. The downstream z/a locations, ranging from 1.2 to 8.1, are denoted by the numbers above each profile. The structural evolution of the shadow begins at $z/a = 1.6$. The evolution of a current enhancement in the boundary regions (see Figure 3) becomes apparent at z/a locations beyond 1.2.

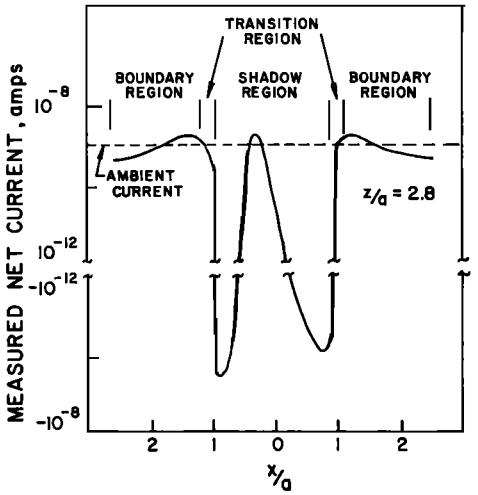

Fig. 3. Transverse current profiles with the three separate regions defined. The figure also shows a comparison at $z/a = 2.8$ of the measured current enhancement downstream of the model and the measured ambient current (without the model). The vertical and horizontal axes are the same as in Figure 2. The profile obtained downstream from the model shows a large current enhancement in the shadow region with a peak current slightly larger than the ambient current. The ambient current profile shows that for a transverse distance greater than $\pm 2a$ the high-energy plasma beam was flat to within $\pm 10\%$ and that there was no noticeable effects in the undisturbed plasma which would account for the large current enhancement in the shadow.

flat to within $\pm 10\%$. Comparison of the two contours in Figure 3 shows that a definite peak is present on the wake center line behind the model and that the amplitude of the peak is slightly larger than the net current recorded for the undisturbed ambient plasma. Figure 3 also shows small net enhancements at the edges of the shadow.

Figure 4 is a plot on an expanded horizontal scale of the measured net current in the transition region of the profile taken at $z/a = 3.8$. The error bars in this figure show the range of the net current fluctuations that occurred at a frequency of less than 30 Hz and were always present in this region when the model was located in the plasma beam. As shown in Figure 4, the turbulence began at the edge of the boundary region and increased with maximum fluctuations (approximately $\pm 70\%$ of the net current) occurring in the region of polarity reversal at the center of the transition region and decreasing as the edge of the shadow was reached. This type of turbulence was seen in the transition regions in all profiles taken downstream from the model. Low level fluctuations ($\pm 10\%$), also with a frequency less than 30 Hz, were observed in the boundary region as well.

Figure 5 shows the measured net current on the wake center line downstream from the model as a function of z/a. These currents were obtained by locating the Langmuir probe at the intersection of the vertical and horizontal center lines and then systematically moving it to increasing z/a locations. This plot emphasizes the presence of the evolving peaks in the measured net current along the wake center line downstream from the model.

Discussion

'Shadow' Region

We define the region directly behind the model as the 'shadow' (see Figure 3). The shadow structure shown in Figure 2 appears to be the major difference between the high-energy solar wind plasma/model interactions presented in this paper and the low-energy plasma/model interactions previously studied by others. Many authors [*Hester and Sonin*, 1969; *Oran et al.*, 1974; *Stone*, 1981*a*, *b*] have reported orderly transitions with increasing z/a from a plasma 'void' in the near wake of a model to an enhancement peak, and then to 'outwards travelling density peaks' at locations where the ratio of z/a to the mach number ($(z/a)/M$, the 'Mach ratio') is greater than one. In contrast, in the case of our higher energy plasma interaction the 'shadow' is very structured at z/a locations where the Mach ratio is less than one and the enhancement peaks have an evolution throughout this region. This evolution of the peak and its associated structuring at these Mach ratios appears to be a permanent feature of the wake in our high energy plasma and may be indicative of the downstream wake of any body in a high speed plasma flow; e.g., a planetary body in the solar wind.

Figure 2 indicates that in the shadow region very close to the model ($z/a < 2.5$) the major feature of the observations is the absence of measurable net positive current and the presence of quite large net negative currents (5×10^{-10} A maximum). This phenomenon was also observed and mentioned in passing by *Hester and Sonin* [1969]. Another feature of the shadow is its narrowness at z/a locations of 1.2 and 1.3. The width of the shadow at $z/a = 1.2$ is approximately 70% of the model diameter increasing to approximately 90% of the model diameter at $z/a = 1.3$. This effect was carefully checked for accuracy.

The plots in Figure 2 clearly indicate that the structuring in the shadow begins at $z/a = 1.6$ and continues to increase in amplitude until at $z/a = 2.8$ an enhancement peak is observed that is slightly greater than the undisturbed (ambient) net positive current at this location (see Figure 3). This peak is bounded on either side by large net negative currents ($\sim 3 \times 10^{-10}$ A). The appearance of the enhancement peak at a Mach ratio of 0.3 when the model is maintained at zero potential is in direct contrast to the data published for low-

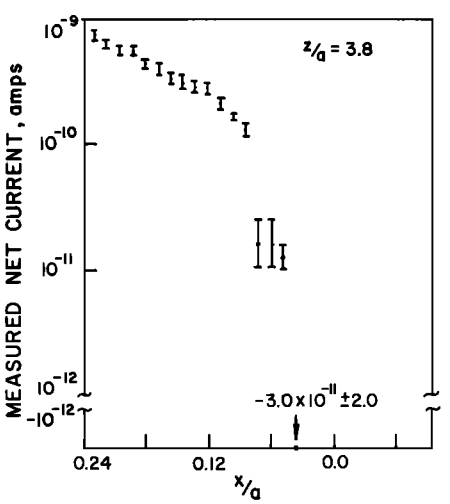

Fig. 4. The 'transition' region measured at $z/a = 3.8$. This plot is typical of the turbulent region in all our profiles. The error bars show the range of the measured net current fluctuations. These fluctuations occurred at a frequency less than 30 Hz and were always present in this region when the model was located in the plasma beam. The vertical axis is the same as that used in Figure 2. The horizontal axis step size has been decreased to show the turbulence measured in this region. The total x/a distance covered by the horizontal axis is only 0.24. There are two such regions in each transverse current profile and they are essentially identical.

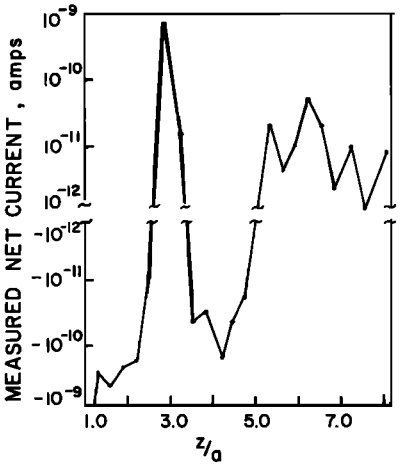

Fig. 5. A plot of the measured net current on the model shadow center line showing the nature of the evolution of the current in the wake. The vertical axis is the same as that used in Figure 2 and the horizontal axis is the dimensionless number z/a.

energy plasma experiments with a body floating at a few kT_e negative potential [*Hester and Sonin*, 1969; *Stone*, 1981*b*], which predict that the enhancement peak should appear at a Mach ratio of approximately one.

In contrast to this maximum enhancement, a decrease is observed in the amplitude of the enhancement peak at z/a = 3.2, where $+8 \times 10^{-12}$ A is measured, bounded by currents of $\sim -1 \times 10^{-10}$ A. The shadow structure continues evolving, at z/a = 3.5 there is a broad central peak (with considerable fine structure) consisting of only measured net negative current. A small net positive current enhancement occurs at z/a = 3.8 (a Mach ratio of 0.42), although it is not symmetric about the model center line. This nonsymmetry of the enhancement peak was also shown to occur at zero volts bias on the model in *Hall et al.* [1964] (see their Figure 11). This second enhancement is in direct contrast to the low-energy experiments that show that with a fixed zero bias on a spherical model there is only one main enhancement peak occurring at a Mach ratio of approximately one. However, multiple enhancements do occur with small positive bias on very small cylinders [*Hester and Sonin*, 1970] and have been theoretically predicted for symmetric models [*Call*, 1969; *Maslennikov and Sigov*, 1965]. At z/a = 4.4 the enhancement has evolved, decreasing in amplitude and consisting of only net measurable negative current with a substructure of a series of smaller peaks. As indicated in Figure 2, the evolution of the enhancements and their associated structures is repeated out to z/a = 8.1.

Figure 2 also shows that as the shadow becomes gradually wider with increasing z/a it also becomes shallower. This compares favorably with the findings of *Hester and Sonin* [1969] and *Fournier and Pigache* [1975]. Figure 5 shows the net measured current on the wake center line as a function of z/a. The evolution of the current structure downstream of the model is evident. These results are similar to the axial density oscillations predicted by *Grabowski and Fischer* [1975] (see their Figure 8).

'Transition' Region

Figure 3 defines the 'transition' region in the profile. This narrow region, in which the net measured current changes from positive to negative values, usually is <0.5 cm wide. It is a very turbulent region with the fluctuations increasing near the center and decreasing towards the edges (see Figure 4). This turbulence appears to be a direct effect of the interaction of the high-speed flow with the model since when the model is removed from the plasma the turbulence is no longer present and there are no indications of changes in the baseline plasma parameters that would account for this type of behavior. One can speculate that turbulence was present in the plasma at all times but that it was masked by the high level of the net ambient currents. To investigate this possibility, we conducted tests with a lower net ambient current level. While maintaining the transverse location of the detector, the model was systematically moved into and out of the plasma, and the respective net currents were recorded. Although a high level of turbulence was present when the model was in the beam, no measurable turbulence was detected in the ambient plasma. Therefore, we conclude that the fluctuations in this region are a direct effect of the interaction of the high-energy plasma with the model. Similar fluctuations at 3.2 kHz were observed in in situ measurements on the Ariel 1 spacecraft [*Samir and Wilmore*, 1965]. Very high frequency oscillations (several mHz) in a steady state laboratory plasma were reported by *Bernstein and Sellen* [1963]. These types of fluctuations may have been overlooked in the other low-energy plasma laboratory experiments and the possibility of their existence should be investigated.

'Boundary' Region

Figure 3 defines the 'boundary' region. The location of the boundary region is a direct function of the distance (z/a) downstream from the model. At z/a = 1.2, the edges of the shadow are located at $x/a \sim \pm 0.9$ from the model center line (see Figure 2). At increasing z/a locations the boundary region moves outward until at z/a = 8.1 the edges of the shadow are observed at $x/a \sim \pm 2$ from the model center line.

Prior to photoreduction the profiles in Figure 2 showed that the boundary region develops a fine structure that becomes a permanent feature of the data beyond z/a = 2.8. Similar fine structure was seen by *Fournier and Pigache* [1975] (see their Figures 10 and 11). Figure 3 also shows that there is a small current enhancement at the edge of the shadow beyond z/a = 1.3 which appears to be a permanent feature of the boundary region in all of our profiles. To further examine and calibrate this effect, the model was removed from the plasma beam after each transverse scan and a profile was taken of the ambient current at each z/a location. These ambient profiles show no increases in current in the regions where enhancements occur when the model is present. Therefore, we attribute this effect to the interaction of the high-energy plasma beam with the model. The density profiles in *Stone* [1981*a*, *b*] show similar edge enhancements in the region where the Mach ratio is less than one. Low amplitude fluctuations ($< \pm 10\%$) with similar characteristics to those seen in the transition region were observed in the boundary region. These fluctuations did not appear in the ambient plasma when the model was removed.

All of these boundary phenomena—increasing width of the boundary region, fine structure, and the net positive current enhancement—are evident in all of our observations. The underlying mechanisms responsible for these phenomena are not known. Similar effects were observed in in situ measurements in the wake of the Ariel 1 spacecraft [*Henderson and Samir*, 1967; *Samir et al.*, 1974]. However, other authors studying the low-energy plasma/model interaction

[*Hester and Sonin*, 1969; *Oran et al.*, 1974; *Stone*, 1981*a*, *b*] have attributed similar phenomena to outwardly moving density peaks. It is possible that a viscous interaction [*Perez-de-Tejada*, 1980] could also give rise to these same features.

CONCLUSIONS

The profiles presented above demonstrate that the high-energy plasma interaction with the model appears to be much more complex than the interaction reported in comparable low-energy plasma experiments. Significant wake phenomena occurred at z/a locations where the ratio of z/a to Mach number (the 'Mach ratio') was less than one. In previously reported low-energy interactions this was a region where the major feature was the absence of measurable ion currents [*Stone*, 1981*b*]. In contrast, we have shown that the high-energy plasma/model interactions produce permanent current structures in this region. *Stone* [1981*b*] discusses how a potential on the model can affect the location of the enhancement. Since our model was maintained at zero potential, he would predict, on the basis of the low-energy studies with a body floating at a few kT_e negative potential, that the enhancement peak would occur further downstream where the Mach ratio is one. Ions might have been deflected into the wake if there were a low-energy tail to our high energy beam or a significant transverse temperature component. However, our initial calibrations of the plasma beam showed that the beam was monoenergetic and that no significant low-energy ions or transverse temperature components were present. Thus we conclude that the existence of structures at z/a locations ranging from 2.8 to 8.1 (Mach ratios <1) is a new phenomenon resulting from the interaction of the high-energy plasma with the model and that they are permanent features of this interaction.

We have shown that some of the same 'wake filling' phenomena, which may be attributed to crossing plasma streams, are seen in both the high energy and low energy interactions We see that at increasing z/a locations downstream the shadow region increases in width and becomes shallower.

We have found a transition region that shows very strong fluctuations. These fluctuations appear to be a permanent feature of the wake and were not present when the model was rotated out of the plasma. We conclude that the fluctuations are a direct result of the interaction of the high-energy plasma and the large model.

Another permanent feature of our profiles is the boundary region. This region shows a small enhancement and low level turbulence in all our profiles beyond a z/a of 1.3 with the model in the beam. The structuring, which is present in the shadow region, appears to a lesser degree in the boundary region. These features may be attributable to either outwardly moving density peaks or to a viscous interaction [*Dryer*, 1970; *Perez-de-Tejada*, 1980].

Stone [1981*a*] pointed out that there still exist many unanswered questions concerning the nature of the midwake and the effects of scale size and test body geometry on the structures in the wake. In the present study we have begun answering some of these questions. We have also shown the feasibility of studying the plasma interactions utilizing high-energy plasma techniques. Additional studies of the high-energy/model interactions should be conducted at Mach ratios greater than one. This would extend the comparative results of the low and high energy plasma/model interactions, which would lead to a fuller understanding of the complex structuring processes present in these interactions.

Although some laboratory studies of the magnetic field/plasma interaction have been performed [*Podgorny*, 1976], more research is needed to understand the effects of magnetic fields in these interactions. Studies employing magnetic fields in conjunction with low- and high-energy plasma beams would contribute to our understanding of the basic physical mechanisms associated with these interactions. In addition, studies that include temporal variations in the incident plasma beam parameters would be useful for understanding the laboratory interactions and extrapolating them to astrophysical situations.

It is tempting to speculate that the substructures and turbulence observed downstream from the model in our laboratory experiments may also be permanent features of the interaction of high-energy solar system and astrophysical plasmas with planetary, lunar, and astrophysical objects. For example, unlike the solar wind/planetary magnetic field interactions at earth and Jupiter, the flow past Venus [*Intriligator and Smith*, 1979] is a solar wind/atmospheric/ionospheric interaction where the convective pressure of the preshocked solar wind is balanced by the ionospheric pressure [*Intriligator and Smith*, 1979]. A relatively small obstacle is formed, the solar wind interacts directly at the ionopause with the ionosphere/atmosphere of the planet, a bow shock is formed upstream, and the postshock heated and compressed solar wind flows past the planet in the ionosheath. This flow past Venus is similar to our laboratory plasma flow past the model. Table 1 summarizes this comparison.

It is possible that there are specific substructures downstream of Venus that may appear transitory or fragmentary owing to the trajectories and orbital characteristics of the spacecraft that traverse them and/or due to the instrumental limitations of flight hardware that probe them. At times these structures may be perturbed owing to temporal variations in the solar wind but, generally on the basis of our laboratory experiments, we suggest that they may be relatively permanent features of the interaction of the solar wind with Venus rather than transitory phenomena attributable to temporal variations in the solar wind.

Acknowledgments. This paper represents one aspect of research carried out at the University of Southern California under NASA grant NGR-05-018-181. J. M. Sellen, Jr., generously participated in the initial phases of work in this plasma facility. Many students at USC participated in the laboratory work. We particularly acknowledge the contributions of R. Dinning and D. Woodruff. The authors are grateful to M. Dryer, U. Samir, and N. Stone for useful discussions of this research.

The Editor thanks R. L. Stenzel and another referee for their assistance in evaluating this paper.

REFERENCES

Bernstein, W., and J. M. Sellen, Jr., Oscillations in synthetic plasma streams, *Phys. Fluids, 6*, 1032, 1963.

Call, S. M., The interaction of a satellite with the ionosphere, *NASA CR-106555*, 1969.

Dryer, M. Solar wind interactions—Hypersonic analogue, *Cosmic Electrodynam., 1*, 115, 1970.

Fournier, G., and D. Pigache, Wakes in collisionless plasma, *Phys. Fluids, 18*, 1443, 1975.

Grabowski, R., and T. Fischer, Theoretical density distribution of plasma streaming around a cylinder, *Planet. Space Sci., 23*, 287, 1975.

Hall, D. F., R. F. Kemp, and J. M. Sellen, Jr., Plasma vehicle interaction in a plasma stream, *AIAA J., 2,* 1032, 1964.

Hall, D. F., R. F. Kemp, and J. M. Sellen, Jr., Generation and characteristics of plasma wind-tunnel streams, *AIAA J., 3,* 1490, 1965.

Henderson, C. I., and U. Samir, Observations of the disturbed region around an ionospheric spacecraft, *Planet. Space Sci., 15,* 1499, 1967.

Hester, S. D., and A. A. Sonin, A laboratory study of the electrodynamic influences on the wakes of ionospheric satellites, *AIAA Pap., 69-673, 1,* 1969.

Intriligator, D. S., and E. J. Smith, Mars in the solar wind, *J. Geophys. Res., 84,* 8427, 1979.

Langmuir, I., and H. Mott-Smith, Jr., Studies of electric discharges in gases at low pressures, *Gen. Electr. Rev., 27,* 449, 1924.

Maslennikov, M. V., and Yu S. Sigov, A discrete model for the study of the flow of a rarefied plasma about a body, *Sov. Phys. Dokl. Engl. Transl., 9,* 1063, 1965.

Oran, W. A., N. H. Stone, and U. Samir, Parametric study of near-wake structure of spherical and cylindrical bodies in the laboratory, *Space Sci., 22,* 379, 1974.

Perez-de-Tejada, H., Viscous flow circulation of the solar wind behind Venus, *Science, 207,* 981, 1980.

Podgorny, I. M., Laboratory experiments plasma intrusion into the magnetic field, in *Physics of Solar Planetary Environments,* vol. 1, edited by D. J. Williams, p. 251, AGU, Washington, D. C., 1976.

Samir, U., and A. P. Wilmore, The distributions of charged particles near a moving spaecraft, *Planet. Space Sci., 13,* 285, 1965.

Samir, U., N. H. Stone, and W. A. Oran, Does a two-stream flow model apply to wakes of large bodies in space?, *Astrophys. Space Sci., 31,* 1974.

Schott, L., Electrical probes, *Plasma Diagnostics,* p. 668, edited by W. Lochte-Holtgreven, North-Holland, Amsterdam, 1968.

Sellen, J. M., Jr., W. Bernstein, and R. F. Kemp, Generation and diagnosis of synthesized plasma streams, *Rev. Sci. Instrum., 36,* 316, 1965.

Stone, N. H., The plasma wake of mesosonic conducting bodies, Part 1, An experimental parametric study of ion focusing by the plasma sheath, *J. Plasma Phys., 25,* 351, 1981*a*.

Stone, N. H., The aerodynamics of bodies in a rarified ionized gas with applications to spacecraft environmental dynamics, *NASA Tech. Pap. 1933,* 1981*b*.

(Received September 30, 1981;
revised April 20, 1982;
accepted April 21, 1982.)